



Actin Is Required for Cellular Development and Virulence of *Botrytis cinerea* via the Mediation of Secretory Proteins

Hua Li,^{a,b} Zhanquan Zhang,^{a,c} Guozheng Qin,^{a,c} Chang He,^{a,b} Boqiang Li,^{a,c} Shiping Tian^{a,b,c}

^aKey Laboratory of Plant Resources, Institute of Botany, The Innovative Academy of Seed Design, Chinese Academy of Sciences, Beijing, China

^bUniversity of Chinese Academy of Sciences, Beijing, China

^cKey Laboratory of Post-Harvest Handling of Fruits, Ministry of Agriculture of China, Beijing, China

Hua Li and Zhanquan Zhang contributed equally to this work. Author order was determined alphabetically.

ABSTRACT Actin is a vital component of the cytoskeleton of living cells and is involved in several complex processes. However, its functions in plant-pathogenic fungi are largely unknown. In this paper, we found that deletion of the *Botrytis cinerea* actin gene *bcactA* reduced growth and sporulation of *B. cinerea* and lowered virulence. Based on iTRAQ (isobaric tags for relative and absolute quantification)-based proteomic analysis, we compared changes of the secretome in $\Delta bcactA$ and wild-type strains. A total of 40 proteins exhibited significant differences in abundance in $\Delta bcactA$ mutants compared with the wild type. These proteins included 11 down-accumulated cell wall-degrading enzymes (CWDEs). Among them, two CWDEs, cellobiohydrolase (BcCBH) and β -endoglucanase (BcEG), were found to contribute to the virulence of *B. cinerea*, indicating that *bcactA* plays a crucial role in regulating the secretion of extracellular virulence factors. These findings unveil previously unknown functions of BcactA to mediate the virulence of *B. cinerea* and provide new mechanistic insights into the role of BcactA in the complex pathogenesis of *B. cinerea*.

IMPORTANCE The cytoskeleton is an important network that exists in cells of all domains of life. In eukaryotic cells, actin is a vital component of the cytoskeleton. Here, we report that BcactA, an actin protein in *B. cinerea*, can affect the growth, sporulation, and virulence of *B. cinerea*. Furthermore, iTRAQ-based proteomic analysis showed that BcactA affects the abundance of 40 extracellular proteins, including 11 down-accumulated CWDEs. Among them, two CWDEs, cellobiohydrolase (BcCBH) and β -endoglucanase (BcEG), contributed to the virulence of *B. cinerea*, indicating that *bcactA* plays a crucial role in regulating extracellular virulence factors. These findings unveil previously unknown functions of BcactA in mediating growth, sporulation, and virulence of *B. cinerea*.

KEYWORDS actin, *Botrytis cinerea*, pathogenesis, secretome

The cytoskeleton is an extremely highly organized but complex and dynamic network that exists in cells of all domains of life, including archaea, bacteria, and eukaryotes. In eukaryotic cells, it is mainly composed of microfilaments, microtubules, and intermediate filaments. Actin is a vital component of microfilaments, and many actin isoforms exist. In mammals, there are three types of actin, namely, α -actin, β -actin, and γ -actin. Deficient mutants of some actin isoforms are lethal, while others are viable. In mice, whole-body β -actin-knockout ($Actb^{-/-}$) mutants are lethal, while whole-body γ -actin-null ($Actg1^{-/-}$) mutants are not (1). In plants, several actin proteins have been discovered. Misexpression of *act1* in vegetative tissues can cause dwarfing of *Arabidopsis thaliana* (2), while the *act2-1* mutant exhibits no phenotypic distinction from the

Citation Li H, Zhang Z, Qin G, He C, Li B, Tian S. 2020. Actin is required for cellular development and virulence of *Botrytis cinerea* via the mediation of secretory proteins. mSystems 5:e00732-19. <https://doi.org/10.1128/mSystems.00732-19>.

Editor Jack A. Gilbert, University of California San Diego

Copyright © 2020 Li et al. This is an open-access article distributed under the terms of the [Creative Commons Attribution 4.0 International license](https://creativecommons.org/licenses/by/4.0/).

Address correspondence to Shiping Tian, tsp@ibcas.ac.cn.

Received 31 October 2019

Accepted 31 January 2020

Published 25 February 2020

wild type (WT) when grown in soil (3). In filamentous fungi, three high-order F-actin structures exist with distinct functions: actin patches, cables, and rings. Actin patches are peripheral punctate structures present at subapical regions, where the endocytic machinery is located (4). The localization of actin patches is indicative of actin's function in endocytosis and exocytosis at the hyphal tip and in coupling those functions to maintain tip growth (5–7). Actin cables predominantly localize at the apex of hyphae and form tracks for myosin V-dependent polarized secretion and organelle transport (8–10). Actin rings participate in septum formation and are essential for cytokinesis in budding yeast and pathogenesis in *Magnaporthe oryzae* (11–13). Actin or actin-related proteins are widely involved in the pathogenicity and secretion of fungi. The F-actin capping protein is important for the hyphal growth and virulence of *Botrytis cinerea* (14). Disruptions of the actin cytoskeleton in *Aspergillus nidulans* can lead to the inhibition of enzyme secretion via blockade of secretory vesicle transportation (15).

B. cinerea is a major phytopathogenic fungus that has been classified as the second most devastating plant pathogen (16). It invades more than 1,000 plant species, particularly fresh horticultural crops, during cultivation, storage, and distribution, leading to huge economic losses of \$10 to \$100 billion annually worldwide (16–18). In the past few years, significant efforts have been focused on effective control by exploring the molecular mechanisms of the pathogenicity of *B. cinerea*. The secretory proteins of *B. cinerea* comprise various virulence factors that facilitate successful host tissue penetration and colonization (19). Our previous studies have shown that *B. cinerea* is able to secrete a variety of enzymes and metabolites that can kill host cells during the infection process (20) and even adjust its secretome in response to changes in ambient pH values (21). The Rab family protein Bcsas1 also plays an important role in hyphal growth and virulence regulation in *B. cinerea* by affecting vesicle transport and protein secretion (22). Therefore, secretome analysis can provide new insights into the role of extracellular proteins in pathogenic invasion. Considering that actin is a cytoskeleton protein reportedly involved in the secretion of enzymes secretion of *A. nidulans* (15), it may also be involved in the secretion of virulence factors in *B. cinerea*. Among the actin proteins, the expression of BcactA was observed to be increased for the first 4 days when bean leaves were inoculated with *B. cinerea* and thereafter decreased (23).

Proteomics have played a dominant role in the study of specific proteins involved in the virulence of plant pathogens (24). Although next-generation and third-generation high-throughput sequencing have developed rapidly and have a strong advantage in determining global changes at the transcription level, they are insufficient in predicting changes at the protein level, because divergence exists between gene transcription and protein expression. Besides gene transcription, protein expression can also be affected by transcription regulation and protein translation (25). In addition, proteomics, such as isobaric tags for relative and absolute quantification (iTRAQ)-based quantitative proteomic analysis, is more efficient in investigating the subproteome, as proteins can be carefully isolated before analysis. We have successfully used proteomics in the past to investigate the subproteome of both nuclear proteins in tomato fruits at different ripening stages (26) and tonoplast proteins in apple fruits at different periods of senescence (27).

In this study, the mutant of the cytoskeleton protein BcactA was constructed. Deletion of *bcactA* resulted in reduced growth rate, sporulation, and virulence of *B. cinerea*. To further unveil the downstream proteins regulated by BcactA, iTRAQ-based quantitative proteomic analysis was conducted. Forty differentially expressed secretory proteins were identified as being associated with the $\Delta bcactA$ mutant. Among them, BcCBH and BcEG were shown to be involved in the regulation of *B. cinerea* virulence. These results reveal a previously unknown function of actin to control both the virulence of a phytopathogen and its associated involved mechanisms.

RESULTS

BcactA is required for vegetative growth and sporulation. The BcactA gene (Bcin16g02020) encodes a conserved actin protein. The amino acid sequence of BcactA

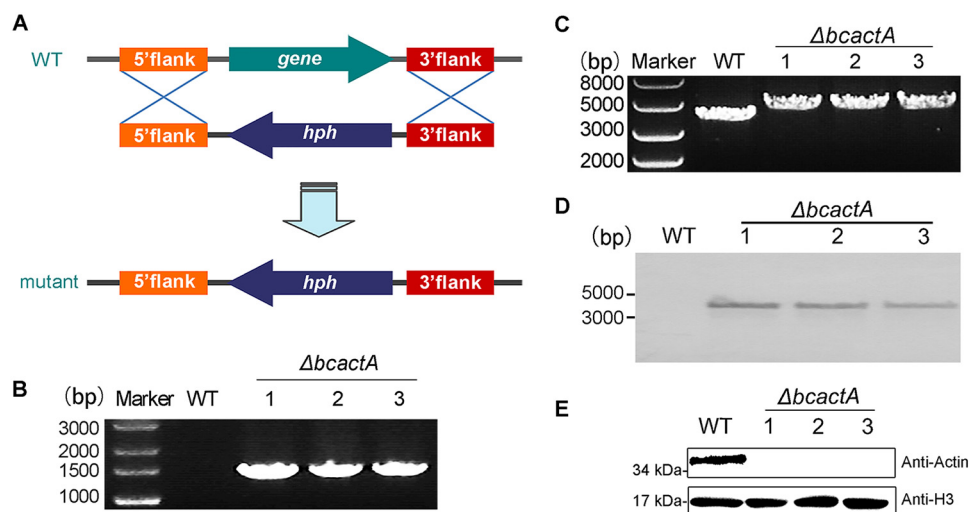


FIG 1 Generation of $\Delta bcactA$ mutants. (A) Replacement strategy for deletion of the *bcactA* gene. The 5' flank and 3' flank of *bcactA* were amplified and ligated into pLOB7 to flank the hygromycin resistance cassette to obtain the replacement vectors. Deletion mutants were generated by replacing the *bcactA* gene with the hygromycin resistance cassette through transformation of the protoplasts of the wild-type (WT) strain. (B) PCR diagnosis of $\Delta bcactA$ mutants. PCR was performed using the primer pair *bcactA*-homo-up/HPH-det, to ensure that homologous recombination occurred at the target site. (C) Diagnosis of the homozygotes of $\Delta bcactA$ mutants. PCR was performed with the primer pair *bcactA*-homo-up/*bcactA*-R-down, to ensure that the mutants were homozygous with no wild-type bands. (D) Southern blot analysis of WT and $\Delta bcactA$ strains. The genomic DNA was digested with *SacI* and *BamHI*, separated in an agarose gel, and hybridized with a probe (a fragment on the hygromycin resistance cassette labeled with digoxigenin). Numbers represent different strains. (E) Immunoblotting analysis of BcactA protein in WT and $\Delta bcactA$ strains. Total cytoplasmic proteins were extracted from 2-day-old mycelia cultured in PDB and immunoblotted with commercially available antibody to actin (Abmart; M20011). Histone 3 (H3) was used as a loading control.

shows high homology with the actin proteins in model organisms (see Fig. S1 in the supplemental material). To investigate the role of BcactA in the growth, colony morphology, and sporulation of *B. cinerea*, a knockout mutant of *bcactA* was generated by replacing the *bcactA* gene (Bcin16g02020) with a hygromycin resistance cassette through transformation of protoplasts of the wild-type strain (Fig. 1A). Three independent transformants were obtained through screening on selection medium supplemented with hygromycin B and subsequent PCR verification (Fig. 1B). After single spore isolation, the transformants were verified by PCR as homozygous (Fig. 1C) and further confirmed to be single-copy insertions by Southern blot analysis (Fig. 1D). To further confirm that the mutant indeed lost the actin protein, we conducted Western blot analysis with a commercial antibody to actin. The results indicated that in the $\Delta bcactA$ knockout mutant, the actin protein was completely lost (Fig. 1E and Fig. S2). To confirm the correlation between the phenotype of the $\Delta bcactA$ mutant and the inactivation of *bcactA*, complemented strains were constructed and verified by PCR (Fig. S3). The growth rate of the $\Delta bcactA$ mutant was reduced compared with that of the wild-type and complemented strains on complete medium (CM). The colony diameter of the mutant exhibited a 34% reduction at 24 h postinoculation (hpi), and a 36% reduction at 48 hpi, relative to the wild-type and complemented strains (Fig. 2B). The hyphae of the $\Delta bcactA$ mutant were more compact than those of the wild-type and complemented strains on CM (Fig. 2A). The sporulation of the $\Delta bcactA$ mutant was significantly reduced. After culture for 10 days on CM, the sporulation of the mutant was only 33% of that of the wild-type and complemented strains (Fig. 2D). The mutant spores were more likely to be distributed around the center of the plates, while the spores of the wild-type and complemented strains were more evenly distributed over the entire plate (Fig. 2C). These results show that BcactA plays a role in the growth, colony morphology, and sporulation of *B. cinerea*.

BcactA participates in regulating the pathogenicity of *B. cinerea*. To determine whether BcactA was involved in the regulation of pathogenicity in *B. cinerea*, apple and

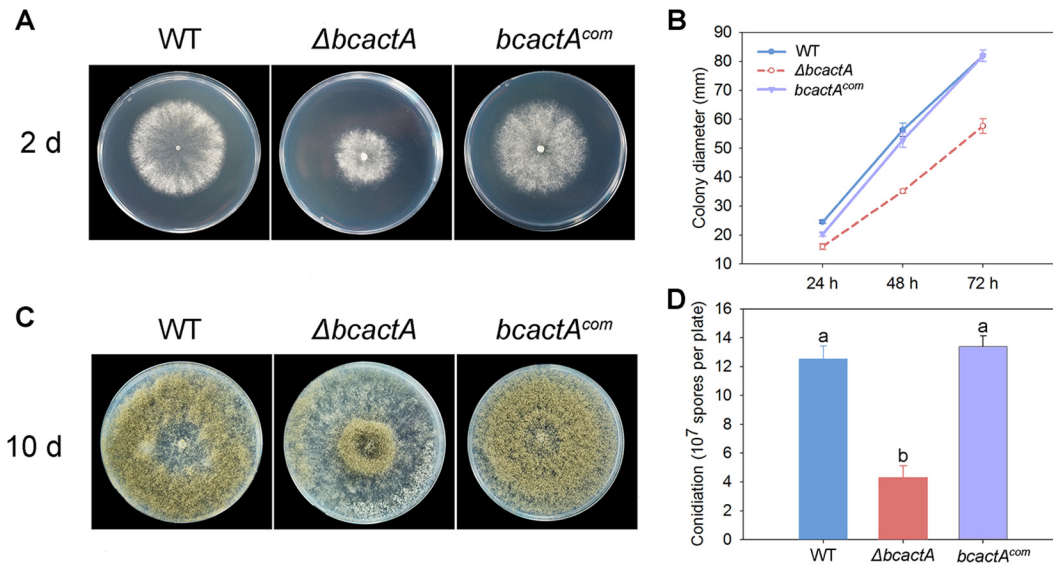


FIG 2 Phenotype detection of $\Delta bcactA$ mutants. (A) Colony morphology of wild-type (WT), $\Delta bcactA$, and $bcactA^{com}$ strains after 48 h of growth on complete medium (CM) plates. (B) Statistical analysis of colony diameter. (C) Sporulation of WT, $\Delta bcactA$, and $bcactA^{com}$ strains after 10 days of growth on CM plates. (D) Statistical analysis of sporulation. Strains were cultured at 22°C. Phenotype detection experiments were repeated three times with similar results, and the pictures shown are representative. Bars represent standard deviations (SD) of the means from three CM plates. Different letters in the same column indicate significant differences ($P < 0.05$).

tomato fruits, as well as detached tomato leaves, were inoculated with the spores of $\Delta bcactA$ mutants. $\Delta bcactA$ mutants exhibited reduced virulence in different hosts (Fig. 3). At 96 hpi, apples inoculated with the $\Delta bcactA1$ mutant showed no lesions, while the WT-inoculated apples showed an average lesion size that reached 11 mm (Fig. 3A). Similarly, considerably reduced lesion sizes were observed in the $\Delta bcactA1$ mutant-inoculated tomato fruits in comparison with the WT-inoculated tomato fruits (Fig. 3B). At 48 hpi, lesion size was approximately 4 mm in the $\Delta bcactA1$ mutant-inoculated tomato leaves, compared with 8 mm in the WT-inoculated tomato leaves (Fig. 3C). The complemented strain of the $\Delta bcactA1$ mutant exhibited almost the same level of virulence as the WT (Fig. 3D). These results show that BcactA plays a role in the pathogenesis of *B. cinerea*.

BcactA affects the contents of extracellular proteins. To investigate the downstream targets of BcactA, extracellular proteins were extracted and iTRAQ-based quantitative proteomic analysis was used to analyze the secretome of the WT and $\Delta bcactA$ strains. Proteins were labeled with iTRAQ isobaric tags and subjected to nano-liquid chromatography–tandem mass spectrometry (nanoLC-MS/MS) analysis (Fig. 4). Totals of 220 and 232 proteins with a global false-discovery rate (FDR) below 1% were identified in the two biological replications, respectively, when searching against the *B. cinerea* protein database. A 2-fold cutoff was used as a determinant for proteins showing a significant change in abundance. The abundances of 58 and 63 proteins showed significant changes in the $\Delta bcactA$ mutant in the two biological replications, respectively, in comparison with the WT (40 proteins in common) (Fig. 5A). The up-accumulated and down-accumulated proteins in $\Delta bcactA$ mutants were classified into different functional categories, according to the blast2go tool, which included cell wall-degrading enzymes (CWDEs), oxidation-reduction proteins, glycosylation proteins, carbohydrate metabolism, resistance-associated proteins, and other functional proteins. The CWDEs were the most highly represented group among the categories (Fig. 5B). The ratios of iTRAQ reporter ion intensities, along with all relevant identification information for the differentially expressed proteins, are listed in Table 1.

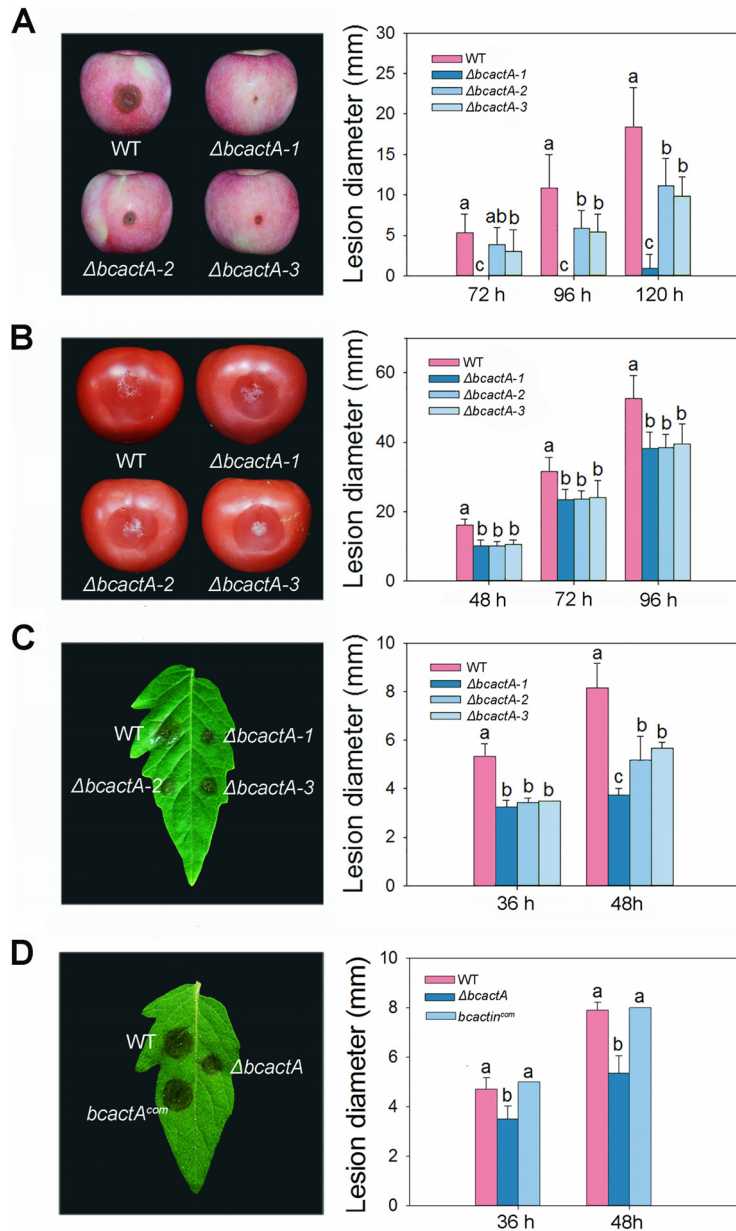


FIG 3 Virulence assays of wild-type (WT), $\Delta bcactA$, and *bcactA^{com}* strains in apple and tomato fruits, as well as detached tomato leaves. (A) Disease symptoms and statistical analysis of WT, $\Delta bcactA1$, $\Delta bcactA2$, and $\Delta bcactA3$ strains on apple fruits. Images were captured after 96 h of inoculation. (B) Disease symptoms and statistical analysis of WT, $\Delta bcactA1$, $\Delta bcactA2$, and $\Delta bcactA3$ strains on tomato fruits. Images were captured after 96 h of inoculation. (C) Disease symptoms and statistical analysis of WT, $\Delta bcactA1$, $\Delta bcactA2$, and $\Delta bcactA3$ strains on detached tomato leaves. Images were captured after 48 h of inoculation. (D) Disease symptoms and statistical results of lesion diameters in detached tomato leaves inoculated with WT, $\Delta bcactA$, and *bcactA^{com}* strains. Images were captured after 48 h of inoculation. Different letters in the same column indicate significant differences ($P < 0.05$).

CWDEs were decreased in $\Delta bcactA$ mutants. To further analyze the 40 differentially expressed proteins identified in the $\Delta bcactA$ mutants, a heat map within each functional category was applied according to the expression patterns of identified proteins (Fig. 5C). Noticeably, 11 CWDEs were down-accumulated, except pectate lyase (BcPL; Bcin15g00520). The 11 CWDEs included mannosidase (BcMAN; Bcin01g05680), α -amylase (BcAMY; Bcin04g06250), glycoside hydrolase (BcGH; Bcin7g02860), β -1,3-exoglucanase (BcEXG; Bcin11g01370), glucoamylase (BcGA; Bcin04g04190), arabinofuranosidase (BcABF; Bcin13g03950), cellobiohydrolase (Bc-

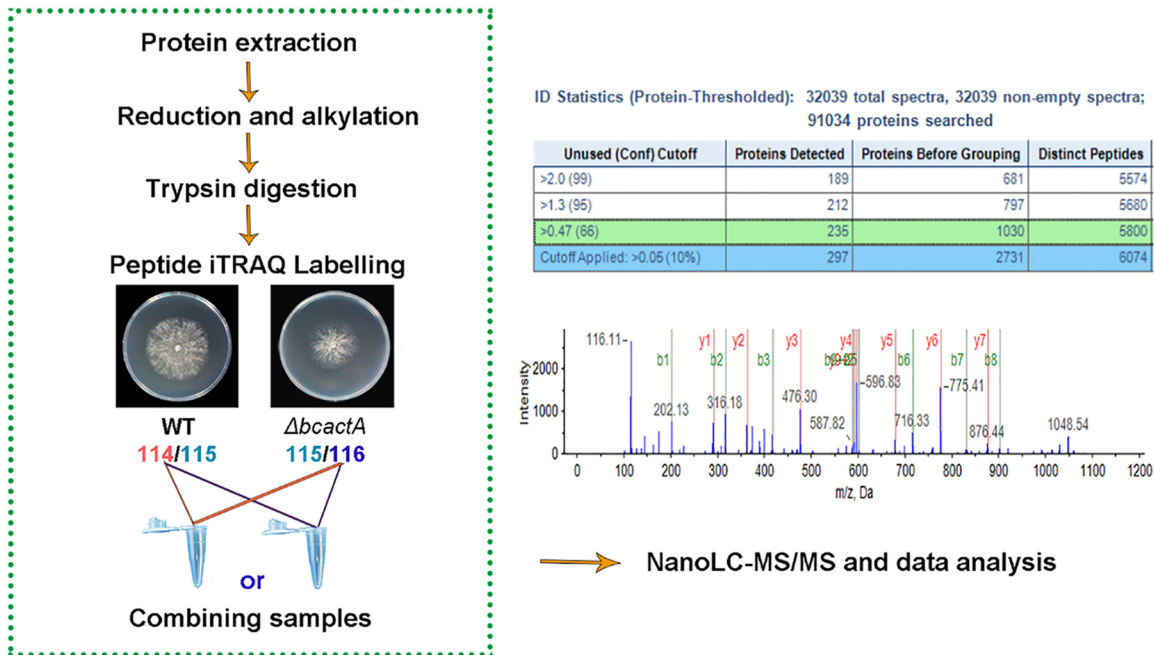


FIG 4 Workflow of quantitative proteomic analysis. Proteins were isolated from wild-type (WT) and $\Delta bcbtA$ mutant strains and subjected to isobaric tags for relative and absolute quantification (iTRAQ) labeling coupled with nanoLC-MS/MS. Two biological repeats were conducted. Images of MS and data analysis were from one repeat.

CBH; Bcin13g02100), endoglucanase (BcEG; Bcin09g00200), β -D-glucan cellobiohydrolase b (BcCBH-b; Bcin16g03950), α -L-rhamnosidase (BcRHA; Bcin01g11040), and esterase (BcEST; Bcin15g00520) (Fig. 5C). These results indicate that BcactA affected the level of CWDEs.

Functional analysis of the identified CWDEs. Among the 11 down-accumulated CWDEs, BcEST reportedly has no effect on the penetration or pathogenicity of *B. cinerea* (28). To further investigate the functions of the other 10 CWDEs (BcMAN, BcAMY, BcGH, BcEXG, BcGA, BcABF, BcCBH, BcEG, BcCBH-b, and BcRHA), knockout mutants of each gene were generated and verified to be homozygous mutants (Fig. S4 and S5). The growth rates of $\Delta bcbtA$, $\Delta bcbtB$, $\Delta bcbtC$, $\Delta bcbtD$, $\Delta bcbtE$, $\Delta bcbtF$, $\Delta bcbtG$, $\Delta bcbtH$, $\Delta bcbtI$, and $\Delta bcbtJ$ mutants were almost the same as that of the WT, and only the growth of the $\Delta bcbtH$ mutant was slower than that of the WT (Fig. 6A). Sporulation of the $\Delta bcbtH$ mutant exhibited a significant reduction; however, that of other mutants showed no significant difference from the WT (Fig. 6B). Similarly, no significant differences were noted in colony morphology of all mutants in comparison with the WT, indicating that BcCBH affected hyphal growth of *B. cinerea*.

BcCBH and BcEG are involved in the regulation of virulence in *B. cinerea*. To evaluate whether the 10 CWDEs were involved in the regulation of virulence of *B. cinerea*, spores of the mutants were collected and inoculated into apple fruits and detached tomato leaves. Compared with the WT-inoculated tomato leaves, lesion diameters were significantly smaller in the $\Delta bcbtH$ mutant-inoculated tomato leaves (Fig. 7B). However, no significant differences were noted in lesion diameters on the $\Delta bcbtH$ mutant-inoculated apple fruits (Fig. 7A). Nevertheless, the $\Delta bcbtG$ mutant exhibited a significant reduction in lesion diameters in the apple fruits (Fig. 7D) but not in detached tomato leaves (Fig. 7E). To confirm that virulence reduction of the mutants was due to the inactivation of corresponding genes, complemented strains were constructed and verified by PCR (Fig. S3). The complemented strains of the $\Delta bcbtH$ and $\Delta bcbtG$ mutants were able to infect tomato leaves and apple fruits at the same rate as the WT (Fig. 7C and F). No significant differences in virulence were observed in other mutants in comparison with the WT (Fig. S6 and S7). These results suggested that two CWDEs, BcCBH and BcEG, were important for the pathogenesis of *B. cinerea*.

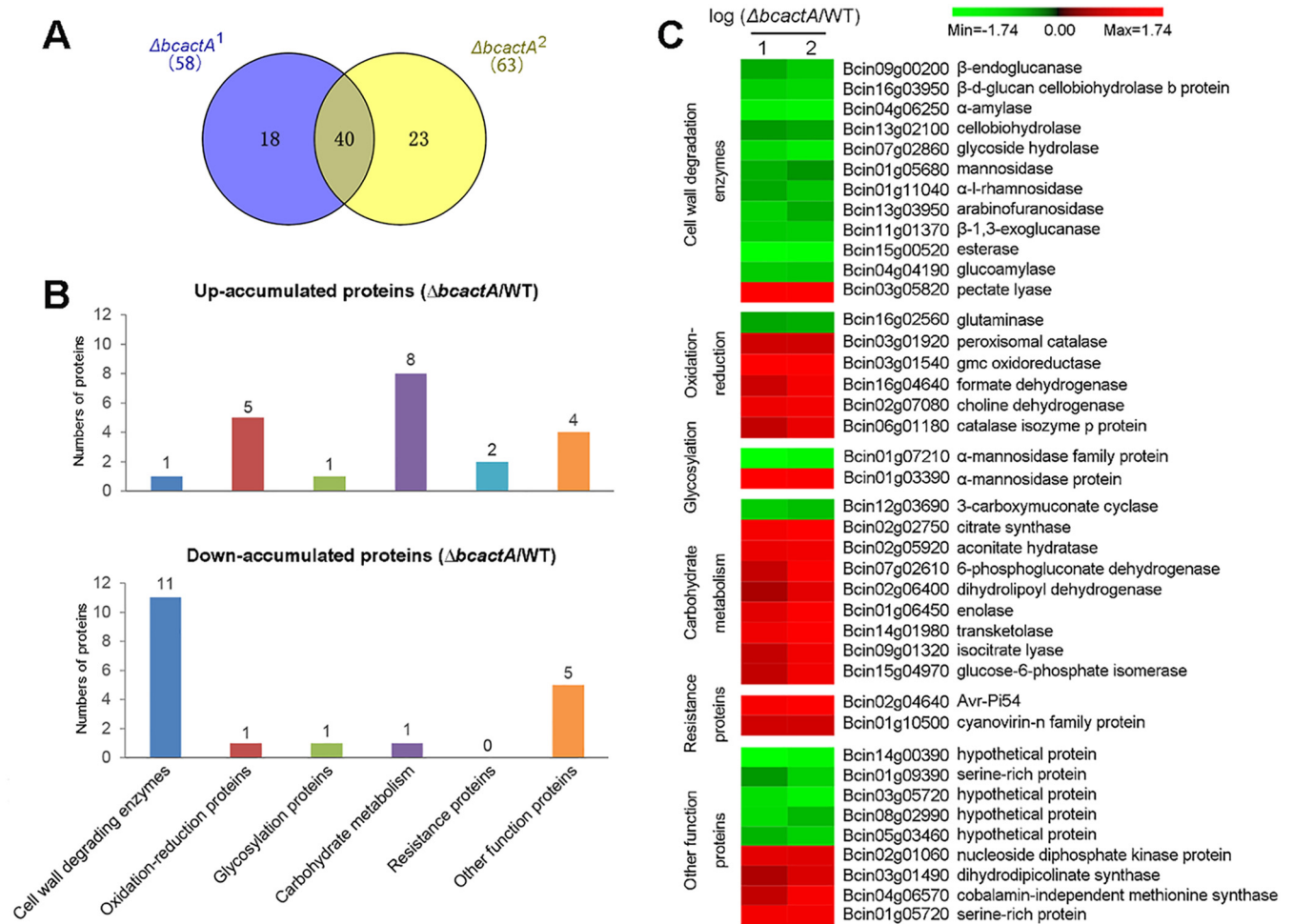


FIG 5 Analysis of differentially accumulated extracellular proteins in $\Delta bcactA$ mutants. (A) Venn diagram of differentially expressed proteins. $\Delta bcactA^1$ refers to the results of the first biological replication, while $\Delta bcactA^2$ refers to the results of the second biological replication. (B) Functional categories of up-accumulated and down-accumulated proteins in $\Delta bcactA$ mutant. (C) Expression patterns of proteins within each functional category. The logarithm of the protein ratio was used to measure the changes in protein abundance. Each row in the color heat map indicates a single protein. The gene identifiers (Bcin numbers) and functional annotations are shown. Red and green colors indicate up-accumulated and down-accumulated proteins, respectively, in $\Delta bcactA$ mutants versus WT.

DISCUSSION

The cytoskeleton of living cells is a highly organized and dynamic network, which plays important roles in various cellular functions, including the regulation of cell polarity, endocytosis, protein secretion, septation, and organelle transport. In fungi, there are three forms of cytoskeleton, filamentous actin, microtubules, and septins, among which actin is a vital component. Actin exists in two forms, G-actin monomers and functional filamentous actin (F-actin). The transition to either of the two forms is closely related to its function (29). An NADPH-oxidase ortholog in yeast, Yno1p, was demonstrated to regulate actin cable formation in yeast cells (30). The regulatory subunit of NADPH-oxidase (NoxR) is required for the formation of a toroidal F-actin structure, which is essential for the protrusion of a rigid penetration peg in *M. oryzae* (11). In our previous study, we found that the protein abundance of actin was affected by NoxR in *B. cinerea* (31). Moreover, gene expression levels of eight NADPH oxidase (NOX) subunits, including *bcnoxR*, were higher in the $\Delta bcactA$ mutant (see Fig. S8 in the supplemental material), indicating that a complex and close association exists between BcnoxR and BcactA. The $\Delta bcactA$ mutant exhibited a reduction in growth rate, sporulation, and virulence in apple and tomato fruits and in detached tomato leaves (Fig. 2 and 3). The visibility of the $\Delta bcactA$ mutant was perhaps due to the functional redundancy of other actin-related proteins or other cytoskeletal forms.

TABLE 1 Differential proteins in $\Delta bcactA$ mutant versus the wild type

Function and accession no. ^a	Protein description	Log ($\Delta bcactA^1:WT$) ^b	Log ($\Delta bcactA^2:WT$) ^c	Unused protein score	Peptide (95%) ^d	% sequence coverage ^e
Cell wall degradation						
Bcin09g00200	β -Endoglucanase	-0.40	-0.57	21.40	24	37.53
Bcin16g03950	β -D-Glucan cellobiohydrolase b protein	-0.62	-0.68	13.63	9	32.44
Bcin04g06250	α -Amylase	-0.95	-1.04	48.98	47	53.20
Bcin13g02100	Cellobiohydrolase	-0.32	-0.38	84.18	81	68.41
Bcin07g02860	Glycoside hydrolase	-0.70	-0.90	8.02	5	15.06
Bcin01g05680	Mannosidase	-0.43	-0.30	17.91	9	16.98
Bcin01g11040	α -L-Rhamnosidase	-0.38	-0.54	33.32	24	32.35
Bcin13g03950	Arabinofuranosidase	-0.62	-0.40	92.26	95	73.12
Bcin11g01370	β -1,3-Exoglucanase	-0.58	-0.61	204.56	215	72.17
Bcin15g00520	Esterase	-1.26	-1.15	17.94	20	48.61
Bcin04g04190	Glucosylase	-0.59	-0.57	83.15	68	59.84
Bcin03g05820	Pectate lyase	1.32	1.32	16.94	16	50.76
Oxidation-reduction						
Bcin16g02560	Glutaminase	-0.47	-0.51	57.49	52	57.68
Bcin03g01920	Peroxisomal catalase	0.78	0.78	33.78	26	43.03
Bcin03g01540	GMC oxidoreductase	1.56	1.65	354.50	418	84.87
Bcin16g04640	Formate dehydrogenase	0.74	1.28	41.14	27	51.72
Bcin02g07080	Choline dehydrogenase	1.14	1.29	131.40	127	57.82
Bcin06g01180	Catalase isozyme P protein	0.66	1.09	80.40	66	60.63
Glycosylation						
Bcin01g07210	α -Mannosidase family protein	-0.71	-0.56	15.71	10	17.53
Bcin01g03390	α -Mannosidase protein	0.68	0.64	23.99	16	16.96
Carbohydrate metabolism						
Bcin12g03690	3-Carboxymuconate cyclase	-0.59	-0.50	0.97	1	4.14
Bcin02g02750	Citrate synthase	1.03	1.29	17.09	11	30.08
Bcin02g05920	Aconitate hydratase	0.88	0.96	20.51	14	19.54
Bcin07g02610	6-Phosphogluconate dehydrogenase	0.54	1.17	16.69	15	25.48
Bcin02g06400	Dihydrolipoyl dehydrogenase	0.38	0.79	16.71	9	22.16
Bcin01g06450	Enolase	0.77	1.17	59.08	42	63.47
Bcin14g01980	Transketolase	0.93	1.30	39.63	22	32.41
Bcin09g01320	Isocitrate lyase	0.54	0.96	18.01	11	24.09
Bcin15g04970	Glucose-6-phosphate isomerase	0.53	0.96	29.94	28	35.70
Resistance associated						
Bcin02g04640	Avr-Pi54 protein	1.45	1.72	153.40	171	84.13
Bcin01g10500	Cyanovirin-N family protein	0.82	0.82	15.09	14	81.13
Other functions						
Bcin14g00390	Hypothetical protein	-1.51	-1.17	29.71	25	34.75
Bcin01g09390	Serine-rich protein	-0.36	-0.72	19.73	15	34.05
Bcin03g05720	Hypothetical protein	-0.86	-1.14	16.00	17	58.71
Bcin08g02990	Hypothetical protein	-0.83	-0.54	38.29	34	46.26
Bcin05g03460	Hypothetical protein	-0.51	-0.72	7.72	7	21.16
Bcin02g01060	Nucleoside diphosphate kinase protein	0.92	0.88	10.10	6	31.22
Bcin03g01490	Dihydrodipicolinate synthase protein	0.47	0.82	2.38	2	7.08
Bcin04g06570	Cobalamin-independent methionine synthase	0.61	1.26	21.30	15	20.60
Bcin01g05720	Serine-rich protein	1.16	1.16	102.30	100	57.48

^aAccession number from Blast search on NCBI.^bThe logarithm of the fold change of protein expression levels in $\Delta bcactA$ mutant versus the wild type from the first independent biological replicate. The meaningful cutoff was fixed at 2-fold corresponding to the logarithm of the iTRAQ ratio of >0.3 for upregulation and <-0.3 for downregulation, as mentioned in Materials and Methods.^cThe logarithm of the fold change of protein expression levels in $\Delta bcactA$ mutant versus the wild type from the second independent biological replicate. The meaningful cutoff was fixed at 2-fold corresponding to the logarithm of the iTRAQ ratio of >0.3 for upregulation and <-0.3 for downregulation, as mentioned in Materials and Methods.^dNumber of unique peptides identified (95% confidence).^eAmino acid sequence coverage for the identified proteins.

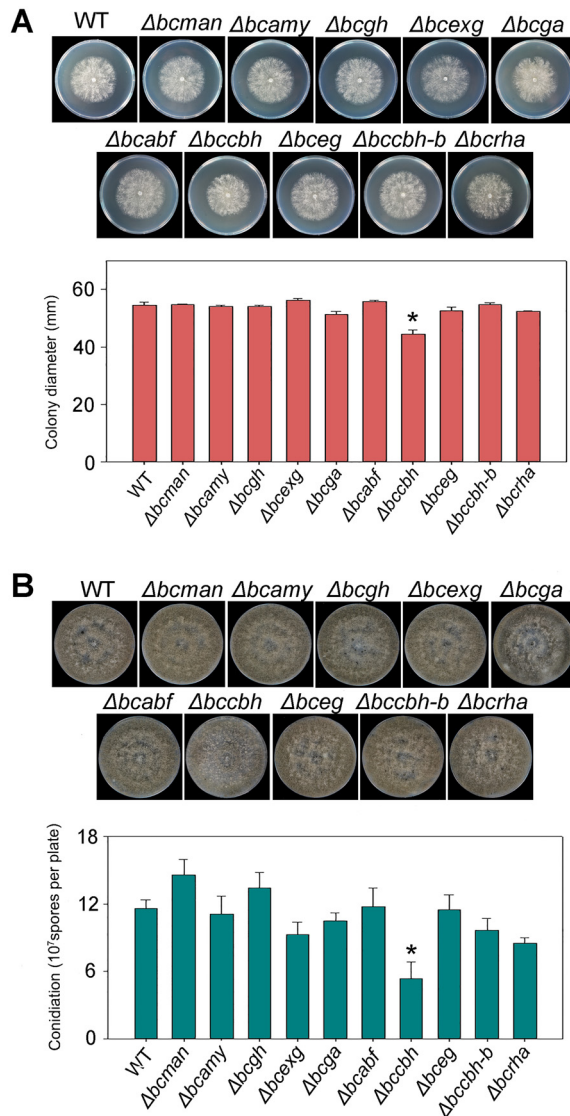


FIG 6 Phenotypic analysis of deletion mutants of 10 cell wall-degrading enzymes (CWDEs). (A) Colony morphology and colony diameters of wild-type (WT) and 10 CWDE mutant strains after 48 h of growth on complete medium (CM) plates. (B) Sporulating cultures and statistical analysis of sporulation of WT and 10 CWDE mutant strains after 10 days of growth on CM plates. Strains were cultured at 22°C. Data presented are the mean \pm SD ($n = 3$). An asterisk indicates a significant difference from the WT ($P < 0.05$). *bcm*, mannosidase; *bcamy*, α -amylase; *bcgh*, glycoside hydrolase; *bcexg*, β -1,3-exoglucanase; *bcga*, glucoamylase; *bcabf*, arabinofuranosidase; *bccbh*, cellobiohydrolase; *bceg*, endoglucanase; *bccbh-b*, β -D-glucan cellobiohydrolase b; *bcrha*, α -L-rhamnosidase.

Actin plays a role in cell motility, maintenance of cell shape, and secretion (32, 33). F-actin cables extend from the plasma membrane into the cell and provide tracks for the targeted delivery of secretory vesicles (32, 33). In pathogenic fungi, the secretory proteins comprise virulence factors that facilitate successful host tissue penetration and colonization (19). Secretory proteins are important for the virulence of *B. cinerea*, as its appressorium is not rigid enough to rupture the host cell wall (34). *B. cinerea* utilizes different secretory proteins to invade host cells, depending on environmental conditions, such as differences in pH values. At pH 4, the secretome of *B. cinerea* favors proteolysis, which is essential for the degradation of the antifungal proteins secreted by the plant host (21, 35). At pH 6, the secretome of *B. cinerea* includes more CWDEs, which are helpful in decomposing the host cell wall to achieve full virulence (21, 36). Therefore, secretome analysis can provide new insights into extracellular protein

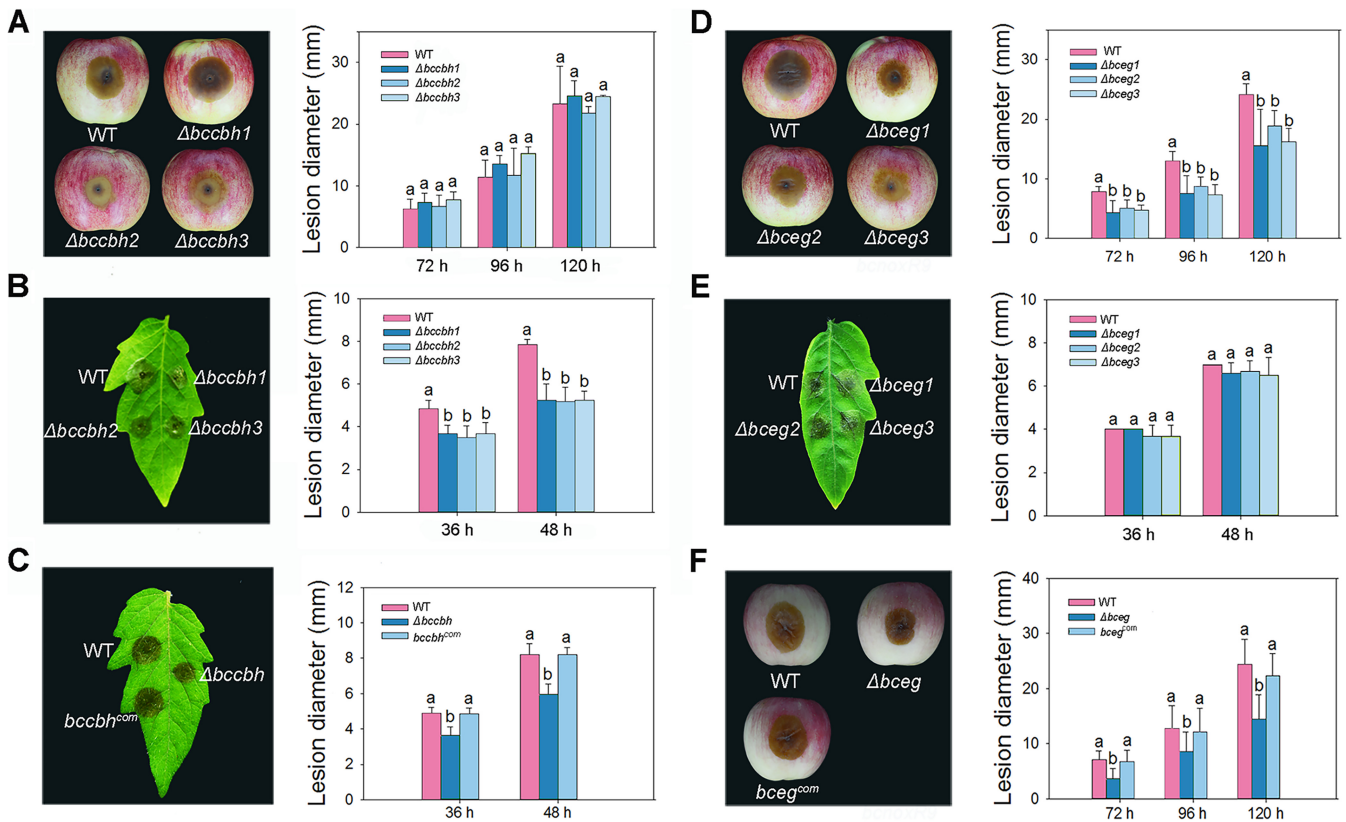


FIG 7 Virulence assays of $\Delta bccb$ and $\Delta bceg$ strains in apple fruits and detached tomato leaves. (A) Disease symptoms (120 hpi) and statistical analysis of WT, $\Delta bccb1$, $\Delta bccb2$, and $\Delta bccb3$ strains in apples. (B) Disease symptoms (48 hpi) and statistical analysis of WT, $\Delta bccb1$, $\Delta bccb2$, and $\Delta bccb3$ strains in detached tomato leaves. (C) Disease symptoms (48 hpi) and statistical analysis of lesion diameters in detached tomato leaves inoculated with WT, $\Delta bccb$, and $bccb^{com}$ strains. (D) Disease symptoms (120 hpi) and statistical analysis of WT, $\Delta bceg1$, $\Delta bceg2$, and $\Delta bceg3$ strains in apples. (E) Disease symptoms (48 hpi) and statistical analysis of WT, $\Delta bceg1$, $\Delta bceg2$, and $\Delta bceg3$ strains in detached tomato leaves. (F) Disease symptoms (120 hpi) and statistical analysis of lesion diameters in apple fruits inoculated with WT, $\Delta bceg$, and $bceg^{com}$ strains. Different letters in the same column indicate significant differences ($P < 0.05$).

function in pathogenic invasion. The iTRAQ-based quantitative proteomic analysis revealed characteristics such as high resolution, high throughput, accurate protein quantification, and repeatability (37). The technique has been used to characterize the dynamic changes of tonoplast proteins during apple fruit senescence (27). In this study, the secretome of the WT and $\Delta bcactA$ strains was examined through iTRAQ-based quantitative proteomic analysis, and 40 differentially expressed proteins were identified in the $\Delta bcactA$ mutant (Fig. 5). These proteins included oxidation-reduction-related proteins, resistance-associated proteins, and cell wall-degrading proteins, among others. Oxidation-reduction proteins are considered to be associated with pathogen invasion, because an oxidative burst usually occurs during infection (34, 38). We identified several oxidation-reduction proteins, including a Cu-Zn superoxide dismutase (Bcin03g03390) that was for the first time determined by proteomics. A deletion mutant of this gene results in reduced virulence in the host (39).

The CWDEs are important in the pathogenesis of phytopathogenic fungi (24). The plant cell wall, which is mainly composed of cellulose, xylan, pectin, and other polysaccharides, is an important barrier for effective defense against phytopathogenic fungi. The composition of the cell wall differs significantly among plant lineages and plant tissues (36). To penetrate the plant cell wall, phytopathogenic fungi produce a diverse array of CWDEs that are capable of degrading the main structural polysaccharide components of the cell wall (40). A total of 1,155 predicted genes encode the enzymes responsible for the creation, modification, or degradation of glycosidic bonds in *B. cinerea*, and 275 of those are predicted to be secretory proteins, as they contain extracellular signal peptide sequences (18). These secretory proteins have been fre-

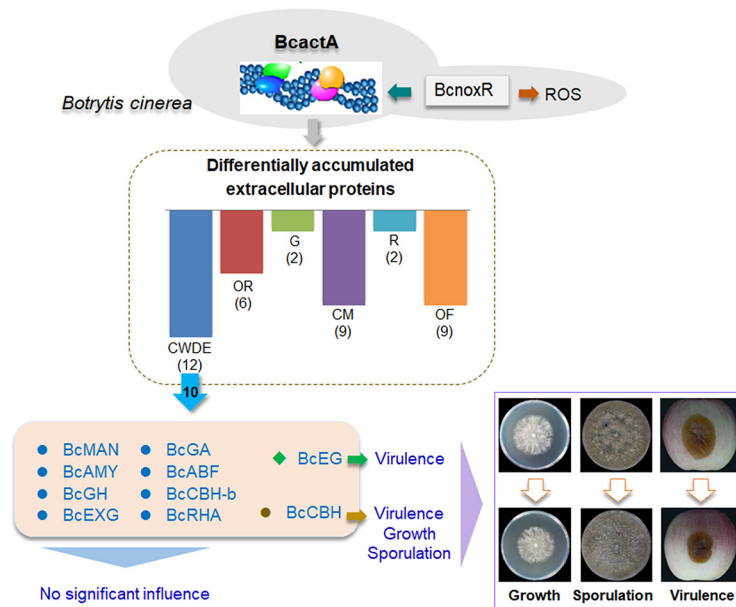


FIG 8 The mode of action of actin (BcactA) regulating the growth, development, and virulence of *B. cinerea*. BcnoXR regulates the actin cytoskeleton, and BcactA affects the secretion of extracellular proteins, which are divided into six groups according to their functions. Among 12 cell wall-degrading proteins, BcCBH is involved in growth, sporulation, and virulence, while BcEG is related to virulence in *B. cinerea*. CWDE, cell wall-degrading enzymes; OR, oxidation-reduction proteins; G, glycosylation proteins; CM, carbohydrate metabolism; R, resistance proteins; OF, other function proteins; BcMAN, mannosidase; BcAMY, α -amylase; BcGH, glycoside hydrolase; BcEXG, β -1,3-exoglucanase; BcGA, glucoamylase; BcABF, arabinofuranosidase; BcCBH, cellobiohydrolase; BcEG, endoglucanase; BcCBH-b, β -D-glucan cellobiohydrolase b; BcRHA, α -L-rhamnosidase; ROS, reactive oxygen species.

quently detected in comparative proteomics and are supposed to be essential virulence proteins (21, 41, 42). A variety of CWDEs have been proven to be essential for the virulence of *B. cinerea*. Endopolygalacturonase 1 (BcPG1) is involved in lesion expansion on apple fruits, tomato fruits, and leaves, while endopolygalacturonase 2 (BcPG2) is involved in both primary infection and lesion expansion of *B. cinerea* on tomato fruits and broad beans (43, 44). In addition, endo- β -1,4-xylanase (BcXYN11A), which can degrade xylan in the plant cell wall, is involved in the virulence of *B. cinerea* (45). In this study, we identified 11 CWDEs that were down-accumulated in the extracellular proteins of the $\Delta b c a c t A$ mutant (Fig. 5C). Cutinase A (BccutA) was previously reported as not essential for penetration of gerbera and tomato (28). The other 10 CWDEs are glycoside hydrolases (GHs), which are mainly associated in cellulose and hemicellulose degradation. We investigated the functions of the 10 GHs encoded by genes associated with growth, morphogenesis, and virulence of *B. cinerea*. The results indicated that two proteins, BcCBH and BcEG, were involved in the virulence of *B. cinerea*. The $\Delta b c c b h$ mutant showed a reduction in growth rate, sporulation, and virulence on detached tomato leaves, while the $\Delta b c e g$ mutant exhibited reduced virulence in apple fruits (Fig. 6 and 7). Other mutants showed almost the same virulence as the wild type, perhaps due to the redundancy of function provided by other enzymes, considering the large number of CWDEs in *B. cinerea*.

In conclusion, we found that the actin protein BcactA mediates growth, development, and virulence of *B. cinerea*, as well as the associated mechanisms. The secretion of a large number of extracellular CWDEs, including some critical virulence factors, is regulated by BcactA, which eventually affects the pathogenicity of *B. cinerea* (Fig. 8). These findings are beneficial for our understanding of the role of BcactA in the complex pathogenesis of *B. cinerea* and provide a novel insight into the regulation network of the actin cytoskeleton.

MATERIALS AND METHODS

Fungal strains and culture conditions. *B. cinerea* (B05.10) was used as the recipient strain for the transformation experiments and as the wild-type control. The wild type and deletion mutants of *B. cinerea* were normally maintained at 22°C on CM, which contained 10 g glucose, 2 g peptone, 1 g yeast extract, 1 g Casamino Acids, 6 g NaNO₃, 0.5 g KCl, 1.11 g MgSO₄·7H₂O, 1.5 g KH₂PO₄, and 0.05 g yeast nitrogen base in 1 liter of distilled water. For collection of spores, the strains of *B. cinerea* were first cultured on CM plates for 1 week at 22°C. Spores were then collected and diluted with sterile distilled water to 1×10^7 spores ml⁻¹, by counting with a hemocytometer under a microscope. For extracellular protein isolation, the spore suspension (1 ml) was added to potato dextrose broth (PDB; which contained 200 g peeled potatoes and 20 g glucose in 1 liter of distilled water) medium (100 ml) and cultured at 22°C for 24 h with shaking at 180 rpm. The mycelium was then harvested using four layers of gauze, washed thoroughly with sterile distilled water, and transferred to modified Czapek medium which contained 1% pectin from apples (Sigma, St. Louis, MO, USA), 0.2% NaNO₃, 0.1% K₂HPO₄, 0.05% KCl, 0.05% MgSO₄·7H₂O, and 0.036 mM FeSO₄·7H₂O. After incubation at 22°C for 72 h with shaking at 180 rpm, the media were filtered with four layers of gauze and used for protein isolation.

Generation of deletion mutants and complemented strains. Approximately 1-kb flanking regions, proximal to the initiation codon and downstream of the termination codons of *bcactA*, *bcman*, *bcamy*, *bcgh*, *bcexg*, *bcga*, *bcabf*, *bccbh*, *bceg*, *bccbh-b*, and *bcrha*, were individually amplified. The amplified PCR products were cloned into pLOB7 (46), verified by sequencing, and introduced into protoplasts of the wild-type B05.10. Protoplast formation and transformation were performed according to the methods of a previous study (22). Briefly, the mycelium was suspended in 20 ml of 0.5% Glucanex solution (Sigma, St. Louis, MO) and incubated at 25°C and 100 rpm for 2 h to generate protoplasts. The transformation fragments were added into a suspension of 200 ml containing 2×10^7 protoplasts. Thereafter 200 μ l and 400 μ l of 25% polyethylene glycol (PEG) 3350 (Sigma) in 50 mM CaCl₂ and 10 mM Tris-HCl (pH 7.5) were added separately. The mixture was then transferred to SH agar, which contained 0.6 M sucrose, 5 mM HEPES, 1 mM (NH₄)₂HPO₄, and 1% agar, to regenerate *B. cinerea* protoplasts. Transformants were initially selected on plates with hygromycin B and then checked using PCR.

Single-spore isolation was conducted to purify the deletion mutants. To verify single-copy genomic integration, Southern blot analysis was performed. Genomic DNA of wild type and three deletion mutants was digested with appropriate restriction enzyme pairs. Southern hybridization was performed with the right flank of the gene as a probe.

For complementation, the DNA fragments of specific genes, along with nucleotides approximately 2 kb upstream and 0.5 to 1 kb downstream, were amplified using wild-type genomic DNA and cloned into the pNAN-OGG vector with resistance to nourseothricin (23). The resulting plasmid was amplified, and the PCR products were used to transform the corresponding mutants. The transformants were initially selected on plates with nourseothricin and then identified by PCR. All primer pairs are listed in Table S1 in the supplemental material.

Isolation of extracellular proteins. Extracellular proteins were isolated according to methods described previously (21). The separated media of wild-type and $\Delta bcactA$ strains were centrifuged three times at $20,000 \times g$ for 30 min at 4°C to remove residual mycelia or other debris. The supernatant was mixed with an equal volume of Tris-HCl (pH 7.5)-buffered phenol by shaking for 30 min at 4°C and centrifuged at $10,000 \times g$ for 40 min to eliminate contaminants. The lower phenol phase was mixed with 5 volumes of 0.1 M ammonium acetate in methanol and incubated at -20°C overnight to precipitate the proteins. Precipitated proteins were separated by centrifugation at $15,000 \times g$ for 30 min at 4°C. The pellet was washed twice with prechilled 0.1 M ammonium acetate in methanol and twice with prechilled acetone. Protein pellets were air dried and stored at -80°C until further use.

iTRAQ labeling and protein identification. For secretome analysis, the extracellular proteins of WT and $\Delta bcactA$ strains were solubilized in the protein buffer, consisting of 100 mM triethylammonium bicarbonate (TEAB) and 0.04% (wt/vol) sodium dodecyl sulfate (SDS), pH 8.5. Protein concentrations were determined using the Bradford assay (47). Sixty micrograms of proteins from each sample was reduced by adding tris-(2-carboxyethyl)phosphine (TCEP) to a final concentration of 10 mM and incubated at 60°C for 1 h. Methyl methanethiosulfonate (MMTS) was added to each sample to a final concentration of 50 mM and incubated at 25°C for 10 min. The samples were then digested with 1.2 μ g trypsin (Promega) at 37°C overnight. The tryptic peptides were labeled with an iTRAQ reagent 4-plex kit (Applied Biosystems) according to the manufacturer's instructions. The iTRAQ tags were able to mark the free amino end. Two independent biological replications were performed. In the first biological replication, the wild-type and $\Delta bcactA$ strains were labeled with iTRAQ tags 114 and 116, respectively. In the other biological replication, the WT and $\Delta bcactA$ strains were labeled with iTRAQ tags 115 and 114, respectively. The labeled samples of each biological replication were separately pooled, vacuum dried, reconstituted in 0.1% formic acid, and submitted for nanoLC-MS/MS analysis.

The mass spectrometry (MS) analysis was performed using a nanoLC system (NanoLC-2D Ultra Plus; Eksigent, USA) coupled with a Triple TOF 5600 Plus mass spectrometer (AB Sciex) (48). The iTRAQ-labeled peptide samples were desalted with a 100- μ m by 20-mm trap column and separated on an analytical 75- μ m by 150-mm column packed with a Magic C₁₈-AQ 5- μ m, 200-Å phase (Michrom). The mobile phase A was 0.1% formic acid in water, while the mobile phase B was 0.1% formic acid in acetonitrile. Peptides were eluted in a linear gradient of 5% to 30% mobile phase B at a flow rate of 300 nl min⁻¹. Precursor ions were selected across the mass range of 350 to 1,500 m/z in high-resolution mode (>30,000). A maximum of 25 precursors per cycle from each MS spectrum were selected for fragmentation with 100-ms minimum accumulation time for each precursor. Tandem mass spectra were recorded in high-sensitivity mode (resolution, >15,000).

Protein identification and quantification were performed using the ProteinPilot 4.5 software (AB Sciex). Mass tolerance for fragment ions was automatically set by the software when using the Triple TOF 5600 Plus mass spectrometer. A database search was performed against the *B. cinerea* protein database with the following parameters: (i) sample type: iTRAQ 4-plex (peptide labeled); (ii) cysteine alkylation: MMTS; (iii) digestion: trypsin; (iv) instrument: Triple TOF 5600; (v) species: none; (vi) quantitate: yes; (vii) bias correction: yes; (viii) background correction: yes; (ix) search effort: thorough; (x) FDR analysis: yes. For iTRAQ quantitation, the peptide for quantification was automatically selected by the Pro Group algorithm (AB Sciex) to calculate the reporter peak area. A reverse database search strategy was applied to estimate the global FDR for peptide identification. Only proteins identified below the 1% global FDR were ultimately exported, and a 2-fold cutoff was used as a determinant for proteins showing a significant change in abundance. A Venn diagram was generated by a web-based Venn diagram software program (<http://bioinfogp.cnb.csic.es/tools/venny/index.html>), and a heat map (Pearson algorithm) was constructed using the PermutMatrix software (version 1.9.3).

Phenotype analysis. For radial growth assays, hyphal disks of the WT and mutants with a diameter of 1 mm were removed from the growing edges. The disks were excised using a cut pipette tip (200 μ l, yellow; Axygen, CA, USA) with an inner diameter of 1 mm. Cultures were grown at 22°C, and measurements were taken daily from 1 to 3 days after inoculation. For sporulation assays, spores were harvested 10 days later using distilled water, and the suspension was filtered through four layers of gauze to remove mycelial fragments. The spores were counted with a hemocytometer under a microscope.

Virulence assays. Spores were harvested by adding sterile water to CM cultures and filtering the mixture through four layers of gauze to remove mycelial fragments. The density of the spore suspension was determined using a hemocytometer under a microscope. Infection assays in tomato and apple fruits were performed according to the methods described in our previous study (49). Tomato and apple fruits were sterilized by immersion in 2% sodium hypochlorite solution for 2 min, rinsed with tap water, and wounded to the same depth (approximately 4 mm) with a sterile nail. Conidia were adjusted to 1×10^4 spores ml^{-1} , and 10 μ l was inoculated into the wounds of apples and tomatoes. Distilled water was used as negative control. Lesion formation was examined at 3 to 5 days after inoculation. For leaf infection assays, conidia were diluted to 2×10^5 spores ml^{-1} with PDB, and 10 μ l was dropped onto tomato leaves harvested from 4-week-old tomato plants. The leaves were placed in moist chambers at 22°C for lesion formation. All experiments were repeated three times, and 15 apples, nine tomatoes and six leaves were used in each replicate.

Western blotting. Total cytoplasmic proteins were extracted from 2-day-old mycelia cultured in PDB, according to methods described previously (29). Protein samples (20 μ g) were separated by 12% SDS-PAGE and then electrotransferred onto a polyvinylidene difluoride (PVDF) membrane by semidry transfer. The membrane was blocked with 5% nonfat milk in phosphate-buffered saline with Tween 20 (PBST) buffer for 1.5 h at room temperature. Immunoblotting was conducted by incubation with a commercially available antibody of actin (Abmart; M20011), produced by immunizing mice with the human actin full-length protein. The immunoreactive bands were visualized by using a chemiluminescence detection kit (SuperSignal; Pierce Biotechnology). Histone 3 (H3) was used as a loading control.

Statistical analysis of data. Statistical differences in phenotype observation and virulence determination experiments were determined using the SPSS software (SPSS Inc., Chicago, IL, USA). One-way analysis of variance (ANOVA) and Tukey's test were used, and a *P* value of <0.05 was considered statistically significant.

SUPPLEMENTAL MATERIAL

Supplemental material is available online only.

FIG S1, TIF file, 2 MB.

FIG S2, TIF file, 0.3 MB.

FIG S3, TIF file, 0.1 MB.

FIG S4, TIF file, 0.3 MB.

FIG S5, TIF file, 0.3 MB.

FIG S6, TIF file, 1 MB.

FIG S7, TIF file, 0.6 MB.

FIG S8, TIF file, 0.2 MB.

TABLE S1, DOCX file, 0.03 MB.

ACKNOWLEDGMENTS

We thank Paul Tudzynski, Julia Schumacher (Westfaelische Wilhelms-Universitaet Muenster, Germany), and Jan van Kan (Wageningen Agricultural University, The Netherlands) for kindly providing the *B. cinerea* haploid strain B05.10 and vectors.

This work was supported by The Key Program of National Natural Science Foundation of China (grants 31930086 and 31530057), The National Key R & D Program of China (2016YFD0400902), and Youth Innovation Promotion Association CAS (2018107).

REFERENCES

- Bunnell T, Burbach B, Shimizu Y, Ervasti J. 2011. β -Actin specifically controls cell growth, migration, and the G-actin pool. *Mol Biol Cell* 22:4047–4058. <https://doi.org/10.1091/mbc.E11-06-0582>.
- Kandasamy MK, McKinney EC, Meagher RB. 2002. Functional nonequivalency of actin isoforms in *Arabidopsis*. *Mol Biol Cell* 13:251–261. <https://doi.org/10.1091/mbc.01-07-0342>.
- Gilliland LU, Kandasamy MK, Pawloski LC, Meagher RB. 2002. Both vegetative and reproductive actin isoforms complement the stunted root hair phenotype of the *Arabidopsis* *act2-1* mutation. *Plant Physiol* 130:2199–2209. <https://doi.org/10.1104/pp.014068>.
- Araujo-Bazán L, Peñalva MA, Espeso EA. 2008. Preferential localization of the endocytic internalization machinery to hyphal tips underlies polarization of the actin cytoskeleton in *Aspergillus nidulans*. *Mol Microbiol* 67:891–905. <https://doi.org/10.1111/j.1365-2958.2007.06102.x>.
- Peñalva MÁ. 2010. Endocytosis in filamentous fungi: Cinderella gets her reward. *Curr Opin Microbiol* 13:684–692. <https://doi.org/10.1016/j.mib.2010.09.005>.
- Shaw BD, Chung D-W, Wang C-L, Quintanilla LA, Upadhyay S. 2011. A role for endocytic recycling in hyphal growth. *Fungal Biol* 115:541–546. <https://doi.org/10.1016/j.funbio.2011.02.010>.
- Takeshita N, Manck R, Grün N, de Vega SH, Fischer R. 2014. Interdependence of the actin and the microtubule cytoskeleton during fungal growth. *Curr Opin Microbiol* 20:34–41. <https://doi.org/10.1016/j.mib.2014.04.005>.
- Fehrenbacher KL, Yang H-C, Gay AC, Huckaba TM, Pon LA. 2004. Live cell imaging of mitochondrial movement along actin cables in budding yeast. *Curr Biol* 14:1996–2004. <https://doi.org/10.1016/j.cub.2004.11.004>.
- Taheri-Talesh N, Xiong Y, Oakley BR. 2012. The functions of myosin II and myosin V homologs in tip growth and septation in *Aspergillus nidulans*. *PLoS One* 7:e31218. <https://doi.org/10.1371/journal.pone.0031218>.
- Taheri-Talesh N, Horio T, Araujo-Bazán L, Dou X, Espeso EA, Peñalva MA, Osmani SA, Oakley BR. 2008. The tip growth apparatus of *Aspergillus nidulans*. *Mol Biol Cell* 19:1439–1449. <https://doi.org/10.1091/mbc.e07-05-0464>.
- Ryder LS, Dagdas YF, Mentlak TA, Kershaw MJ, Thornton CR, Schuster M, Chen J, Wang Z, Talbot NJ. 2013. NADPH oxidases regulate septin-mediated cytoskeletal remodeling during plant infection by the rice blast fungus. *Proc Natl Acad Sci U S A* 110:3179–3184. <https://doi.org/10.1073/pnas.1217470110>.
- Harris SD, Morrell JL, Hamer JE. 1994. Identification and characterization of *Aspergillus nidulans* mutants defective in cytokinesis. *Genetics* 136:517–532.
- Rasmussen CG, Glass NL. 2005. A Rho-type GTPase, rho-4, is required for septation in *Neurospora crassa*. *Eukaryot Cell* 4:1913–1925. <https://doi.org/10.1128/EC.4.11.1913-1925.2005>.
- González-Rodríguez VE, Garrido C, Cantoral JM, Schumacher J. 2016. The F-actin capping protein is required for hyphal growth and full virulence but is dispensable for septum formation in *Botrytis cinerea*. *Fungal Biol* 120:1225–1235. <https://doi.org/10.1016/j.funbio.2016.07.007>.
- Torralba S, Raudaskoski M, Pedregosa AM, Laborda F. 1998. Effect of cytochalasin A on apical growth, actin cytoskeleton organization and enzyme secretion in *Aspergillus nidulans*. *Microbiology* 144:45–53. <https://doi.org/10.1099/00221287-144-1-45>.
- Dean R, van Kan JAL, Pretorius ZA, Hammond-Kosack KE, Pietro AD, Spanu PD, Rudd JJ, Dickman M, Kahmann R, Ellis J. 2012. The top 10 fungal pathogens in molecular plant pathology. *IMA Fungus* 13:414–430. <https://doi.org/10.1111/j.1364-3703.2011.00783.x>.
- Weiberg A, Wang M, Lin FM, Zhao H, Zhang Z, Kaloshian I, Huang HD, Jin HL. 2013. Fungal small RNAs suppress plant immunity by hijacking host RNA interference pathways. *Science* 342:118–123. <https://doi.org/10.1126/science.1239705>.
- Fillinger S, Elad Y. 2016. *Botrytis*—the fungus, the pathogen and its management in agricultural systems. Springer International Publishing, Cham, Switzerland.
- Girard V, Dieryckx C, Job C, Job D. 2013. Secretomes: the fungal strike force. *Proteomics* 13:597–608. <https://doi.org/10.1002/pmic.201200282>.
- Qin GZ, Zong YY, Chen QL, Hua DL, Tian SP. 2010. Inhibitory effect of boron against *Botrytis cinerea* on table grapes and its possible mechanisms of action. *Int J Food Microbiol* 138:145–150. <https://doi.org/10.1016/j.ijfoodmicro.2009.12.018>.
- Li BQ, Wang WH, Zong YY, Qin GZ, Tian SP. 2012. Exploring pathogenic mechanisms of *Botrytis cinerea* secretome under different ambient pH based on comparative proteomic analysis. *J Proteome Res* 11:4249–4260. <https://doi.org/10.1021/pr300365f>.
- Zhang ZQ, Qin GZ, Li BQ, Tian SP. 2014. Knocking out Bcsa1 in *Botrytis cinerea* impacts growth, development, and secretion of extracellular proteins, which decreases virulence. *Mol Plant Microbe Interact* 27:590–600. <https://doi.org/10.1094/MPMI-10-13-0314-R>.
- Schumacher J. 2012. Tools for *Botrytis cinerea*: new expression vectors make the gray mold fungus more accessible to cell biology approaches. *Fungal Genet Biol* 49:483–497. <https://doi.org/10.1016/j.fgb.2012.03.005>.
- Qin GZ, Tian SP, Chan ZL, Li BQ. 2007. Crucial role of antioxidant proteins and hydrolytic enzymes in pathogenicity of *Penicillium expansum* analysis based on proteomics approach. *Mol Cell Proteomics* 6:425–438. <https://doi.org/10.1074/mcp.M600179-MCP200>.
- Pradet-Balade B, Boulmé F, Beug H, Müllner EW, Garcia-Sanz JA. 2001. Translation control: bridging the gap between genomics and proteomics? *Trends Biochem Sci* 26:225–229. [https://doi.org/10.1016/S0968-0004\(00\)01776-X](https://doi.org/10.1016/S0968-0004(00)01776-X).
- Wang YY, Wang WH, Cai JH, Zhang YR, Qin GZ, Tian SP. 2014. Tomato nuclear proteome reveals the involvement of specific E2 ubiquitin-conjugating enzymes in fruit ripening. *Genome Biol* 15:548. <https://doi.org/10.1186/s13059-014-0548-2>.
- Liu RL, Wang YY, Qin GZ, Tian SP. 2016. iTRAQ-based quantitative proteomic analysis reveals the role of the tonoplast in fruit senescence. *J Proteomics* 146:80–89. <https://doi.org/10.1016/j.jprot.2016.06.031>.
- van Kan JA, van't Klooster JW, Wagemakers CA, Dees DC, van der Vlugt-Bergmans CJ. 1997. Cutinase A of *Botrytis cinerea* is expressed, but not essential, during penetration of gerbera and tomato. *Mol Plant Microbe Interact* 10:30–38. <https://doi.org/10.1094/MPMI.1997.10.1.30>.
- Pollard TD, Cooper JA. 2009. Actin, a central player in cell shape and movement. *Science* 326:1208–1212. <https://doi.org/10.1126/science.1175862>.
- Rinnerthaler M, Büttner S, Laun P, Heeren G, Felder TK, Klinger H, Weinberger M, Stolze K, Grousl T, Hasek J, Benada O, Frydlova I, Klockner A, Simon-Nobbe B, Jansko B, Breitenbach-Koller H, Eisenberg T, Gourlay CW, Madeo F, Burhans WC, Breitenbach M. 2012. Yno1p/Aim14p, a NADPH-oxidase ortholog, controls extramitochondrial reactive oxygen species generation, apoptosis, and actin cable formation in yeast. *Proc Natl Acad Sci U S A* 109:8658–8663. <https://doi.org/10.1073/pnas.1201629109>.
- Li H, Zhang ZQ, He C, Qin GZ, Tian SP. 2016. Comparative proteomics reveals the potential targets of BcNoxR, a putative regulatory subunit of NADPH oxidase of *Botrytis cinerea*. *Mol Plant Microbe Interact* 29:990–1003. <https://doi.org/10.1094/MPMI-11-16-0227-R>.
- Dominguez R, Holmes KC. 2011. Actin structure and function. *Annu Rev Biophys* 40:169–186. <https://doi.org/10.1146/annurev-biophys-042910-155359>.
- De Lisle RC. 2015. Role of the actin cytoskeleton in acinar cell protein secretion. *Pancreapedia: exocrine pancreas knowledge base*. <https://www.pancreapedia.org/reviews/role-of-actin-cytoskeleton-in-acinar-cell-protein-secretion>.
- Choquer M, Fournier E, Kunz C, Levis C, Pradier J-M, Simon A, Viaud M. 2007. *Botrytis cinerea* virulence factors: new insights into a necrotrophic and polyphagous pathogen. *FEMS Microbiol Lett* 277:1–10. <https://doi.org/10.1111/j.1574-6968.2007.00930.x>.
- ten Have A, Dekkers E, Kay J, Phylip LH, van Kan JA. 2004. An aspartic proteinase gene family in the filamentous fungus *Botrytis cinerea* contains members with novel features. *Microbiology* 150:2475–2489. <https://doi.org/10.1099/mic.0.27058-0>.
- Kubicek CP, Starr TL, Glass NL. 2014. Plant cell wall-degrading enzymes and their secretion in plant-pathogenic fungi. *Annu Rev Phytopathol* 52:427–451. <https://doi.org/10.1146/annurev-phyto-102313-045831>.
- Chai Y, Zhao M. 2017. iTRAQ-based quantitative proteomic analysis of the inhibitory effects of polysaccharides from *viscum coloratum* (Kom.) nakai on HepG2 cells. *Sci Rep* 7:4596. <https://doi.org/10.1038/s41598-017-04417-x>.
- van Kan JA. 2006. Licensed to kill: the lifestyle of a necrotrophic plant pathogen. *Trends Plant Sci* 11:247–253. <https://doi.org/10.1016/j.tplants.2006.03.005>.
- Rolke Y, Liu S, Quidde T, Williamson B, Schouten A, Weltring KM, Siewers

- V, Tenberge KB, Tudzynski B, Tudzynski P. 2004. Functional analysis of H₂O₂-generating systems in *Botrytis cinerea*: the major Cu-Zn-superoxide dismutase (BCSOD1) contributes to virulence on French bean, whereas a glucose oxidase (BCGOD1) is dispensable. *Mol Plant Pathol* 5:17–27. <https://doi.org/10.1111/j.1364-3703.2004.00201.x>.
40. Tian SP, Torres R, Ballester A, Li BQ, Vilanova L, González-Candelas L. 2016. Molecular aspects in pathogen-fruit interactions: virulence and resistance. *Postharvest Biol Technol* 122:11–21. <https://doi.org/10.1016/j.postharvbio.2016.04.018>.
41. Shah P, Atwood JA, Orlando R, El Mubarek H, Podila GK, Davis MR. 2009. Comparative proteomic analysis of *Botrytis cinerea* secretome. *J Proteome Res* 8:1123–1130. <https://doi.org/10.1021/pr8003002>.
42. Espino JJ, Gutiérrez-Sánchez G, Brito N, Shah P, Orlando R, González C. 2010. The *Botrytis cinerea* early secretome. *Proteomics* 10:3020–3034. <https://doi.org/10.1002/pmic.201000037>.
43. Have A, Mulder W, Visser J, van Kan JA. 1998. The endopolygalacturonase gene Bcpg1 is required for full virulence of *Botrytis cinerea*. *Mol Plant Microbe Interact* 11:1009–1016. <https://doi.org/10.1094/MPMI.1998.11.10.1009>.
44. Kars I, Krooshof GH, Wagemakers L, Joosten R, Benen JA, Van Kan JA. 2005. Necrotizing activity of five *Botrytis cinerea* endopolygalacturonases produced in *Pichia pastoris*. *Plant J* 43:213–225. <https://doi.org/10.1111/j.1365-3113X.2005.02436.x>.
45. Brito N, Espino JJ, González C. 2006. The endo- β -1,4-xylanase Xyn11A is required for virulence in *Botrytis cinerea*. *Mol Plant Microbe Interact* 19:25–32. <https://doi.org/10.1094/MPMI-19-0025>.
46. Zhang LS, Thiewes H, van Kan JA. 2011. The -galacturonic acid catabolic pathway in *Botrytis cinerea*. *Fungal Genet Biol* 48:990–997. <https://doi.org/10.1016/j.fgb.2011.06.002>.
47. Bradford MM. 1976. A rapid and sensitive method for the quantitation of microgram quantities of protein utilizing the principle of protein-dye binding. *Anal Biochem* 72:248–254. [https://doi.org/10.1016/0003-2697\(76\)90527-3](https://doi.org/10.1016/0003-2697(76)90527-3).
48. Wang WH, Cai JH, Wang PW, Tian SP, Qin GZ. 2017. Post-transcriptional regulation of fruit ripening and disease resistance in tomato by the vacuolar protease SIVPE3. *Genome Biol* 18:47. <https://doi.org/10.1186/s13059-017-1178-2>.
49. Zhang ZQ, Qin GZ, Li BQ, Tian SP. 2014. Infection assays of tomato and apple fruit by the fungal pathogen *Botrytis cinerea*. *Bio Protoc* 4:e1311. <https://doi.org/10.21769/BioProtoc.1311>.